An analysis of fully polarimetric W-band ISAR imagery on seven scale model main battle tanks for use in target recognition.

Thomas M. Goyette[*a], Jason C. Dickinson[a], Robert H. Giles[a], William T. Kersey[a], Jerry Waldman[a], William E. Nixon[b]

[a]Submillimeter-Wave Technology Laboratory, University of Massachusetts Lowell, 175 Cabot St., Lowell, MA 01854

[b]U.S. Army National Ground Intelligence Center, 2055 Boulders Road, Charlottesville, VA 22911

ABSTRACT

Fully polarimetric high-resolution W-Band target signature data has been collected on 7 high fidelity1/16th scale model main battle tanks. Data has been collected at several different elevation angles and target poses. Additionally, targets have been measured both on 1/16th scale simulated ground terrain and in free-space. ISAR images were formed from this data for use in several different target identification algorithms. These algorithms include using the data in both linear and circular polarization. The results of the inter-comparisons of the data using different algorithms are presented. Where possible the data has been compared with existing W-Band full-scale field measurements. The data is taken using a 1.55THz compact range designed to model W-Band. The 1.55THz transceiver uses two high-stability optically pumped far-infrared lasers, microwave/laser Schottky diode side-band generation for frequency sweep, and a pair of Schottky diode receivers for coherent integration.

Keywords: Sub-millimeter, Radar, Imagery, Modeling.

1. INTRODUCTION

There is a growing interest in high-resolution, fully polarimetric target signature data for use in automatic target recognition (ATR). In recent years, the U. S. Army National Ground Intelligence Center (NGIC) and the Submillimeter-Wave Technology Laboratory (STL) at the University of Massachusetts Lowell have been developing a database of these measurements at X-band, Ka-band and most recently W-band. NGIC/STL have developed a number of indoor compact ranges to measure the radar cross-section (RCS) of 1/16th scale model targets. Compact ranges have proven their usefulness in the ability to measure targets under controllable conditions. This allows for the rapid collection of data for targets with various poses and ground conditions.

Advances in technology have made high frequency radar systems more common. Research in W-band radar has been of interest because the physical size of the components can be made smaller at these frequencies. Additionally, the angular integration required to form an ISAR image is also much smaller, typically on the order of 0.5˚. Therefore, W-band radar has the advantage of being able to form a high resolution ISAR image without the need to view the target over a wide range of angles.

To investigate the usefulness of W-band data for ATR, seven 1/16th scale model main battle tanks (MBTs) have been studied using the new 1.55 THz W-band compact range. A study of the ISAR cross-correlation is currently being performed using various template and test imaging techniques. The results for the linear HH polarization are presented here.

[*] Correspondence: Email: Thomas_Goyette@uml.edu; Telephone: (978) 458-3807; Fax: (978) 452-3333.

Report Documentation Page

Form Approved
OMB No. 0704-0188

1. REPORT DATE	2. REPORT TYPE	3. DATES COVERED
AUG 2002		**00-00-2002 to 00-00-2002**

4. TITLE AND SUBTITLE	5a. CONTRACT NUMBER
An analysis of full polarimetric W-band ISAR imagery on seven scale model main battle tanks for use in target recognition	5b. GRANT NUMBER
	5c. PROGRAM ELEMENT NUMBER
6. AUTHOR(S)	5d. PROJECT NUMBER
	5e. TASK NUMBER
	5f. WORK UNIT NUMBER
7. PERFORMING ORGANIZATION NAME(S) AND ADDRESS(ES) **University of Massachusetts Lowell,Submillimeter-Wave Technology Laboratory,175 Cabot Street,Lowell,MA,01854**	8. PERFORMING ORGANIZATION REPORT NUMBER
9. SPONSORING/MONITORING AGENCY NAME(S) AND ADDRESS(ES)	10. SPONSOR/MONITOR'S ACRONYM(S)
	11. SPONSOR/MONITOR'S REPORT NUMBER(S)

12. DISTRIBUTION/AVAILABILITY STATEMENT
Approved for public release; distribution unlimited

13. SUPPLEMENTARY NOTES

14. ABSTRACT

15. SUBJECT TERMS

16. SECURITY CLASSIFICATION OF:			17. LIMITATION OF ABSTRACT	18. NUMBER OF PAGES	19a. NAME OF RESPONSIBLE PERSON
a. REPORT **unclassified**	b. ABSTRACT **unclassified**	c. THIS PAGE **unclassified**		**9**	

2. THE 1.55THZ COMPACT RADAR RANGE

The 1.55THz W-band compact range has been described previously[1] and will be only briefly described here. To model W-Band at 16th scale a very high stability 1.55THz laser has been developed. Figure 1 shows the diagram of the 1.55THz compact range. The source consists of two 150 Watt, ultra-stable, grating-tunable CO_2 lasers, which are used as the optical pumps for the two far-infrared lasers. The CO_2 lasers are set to produce 9μm (9P22 CO_2 laser line) and 10μm (10R10 CO_2 laser line) wavelengths respectively. The output of these lasers are then used to pump the laser transitions in the molecular gases difluoromethane (CH_2F_2) and methanol (CH_3OH) at 1.5626THz and 1.5645THz respectively.

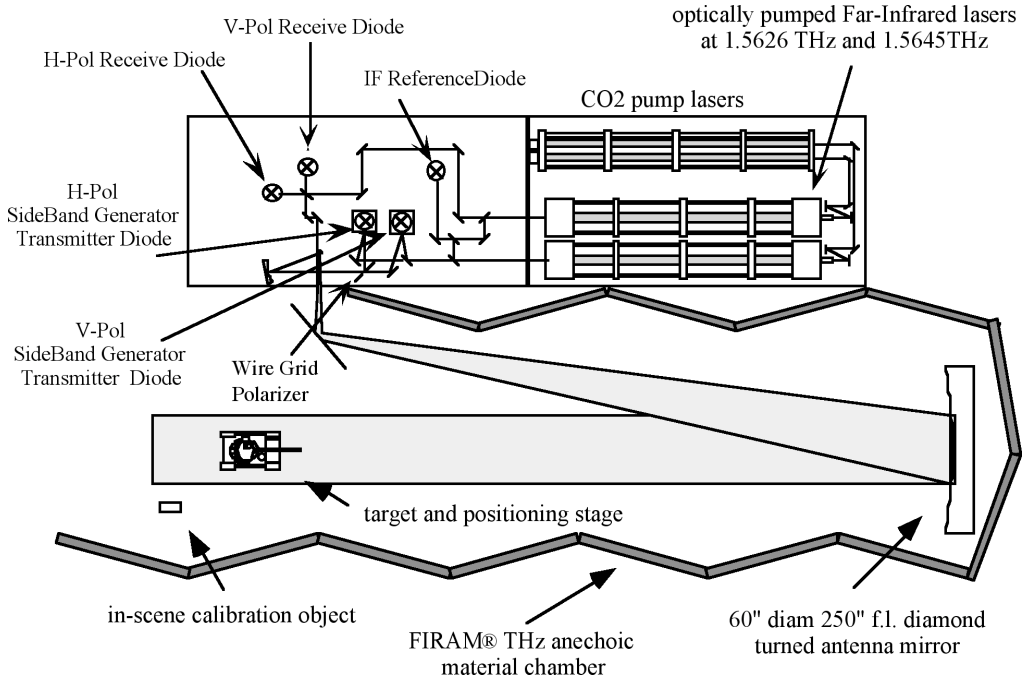

Figure 1. Diagram of the 1.55THz compact radar range.

Frequency tunability is added by electronically combining the output of the lasers with that of a microwave sweeper. This is done by using Schottky diodes as the mixer elements and filtering out the radiated sideband power. The resulting electromagnetic radiation illuminates a 16th scale model mounted on a low cross-section pylon in the compact range. The radar parameters of the 1.55THz compact range are listed in Table 1 along with the full-scale equivalent parameters. The compact range models a fully polarimetric 96.6GHz radar with 11.6" range resolution.

1.55THz Compact Range	**(Full Scale)**
1546 GHz Start Frequency	(96.6 GHz Full scale)
8 GHz Bandwidth	(500 MHz Full Scale)
0.74" Range Resolution	(11.6" Full Scale)
20" Two Way Beam Width	(26.6' Full Scale)
Far Field Beam, 0.3˚ bistatic	
Fully Polarimetric HH, HV, VH, VV amplitude and phase	

Table 1. Radar parameters for the 1.55THz W-band compact range.

3. Results

3.1. Signature measurements and target description.

Seven scale model main battle tanks were measured in this study at an elevation angle of 20˚, and from –5˚ to 365˚ in azimuth angle. Figures 2 and 3 show typical examples of the high quality scale models and the full-scale vehicles on which they were based. The scale model T72 main battle tanks shown in these figures were specifically designed to "fingerprint" the full-scale vehicles. In a previous study of target signature data at Ka-band[2] the accuracy of the models were found to be sufficient to produce very good matches in a comparison of scale model data to full-scale data. A list of the targets that were measured and the measurement conditions is given in Table 2.

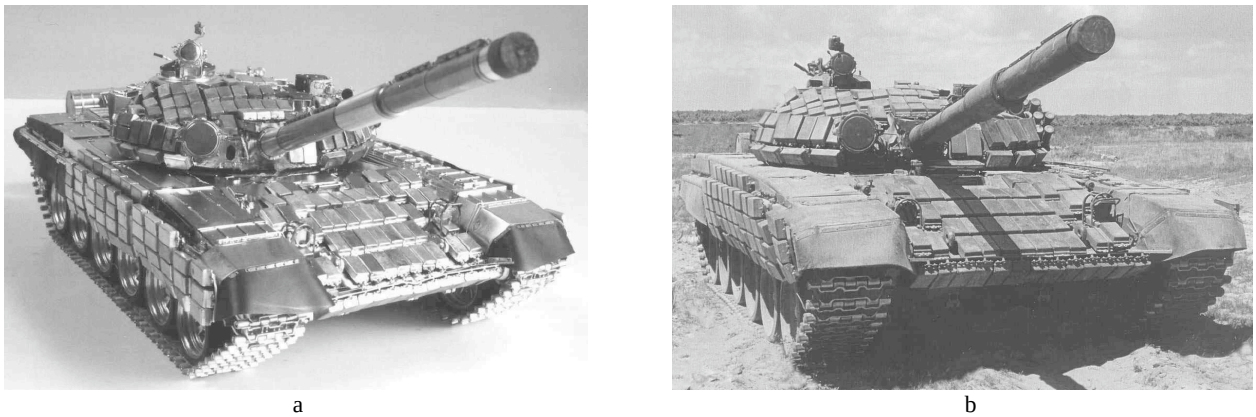

a b

Figure 2. (a) Scale model of the T72 main battle tank with reactive armor (b) the full-scale vehicle on which it was based.

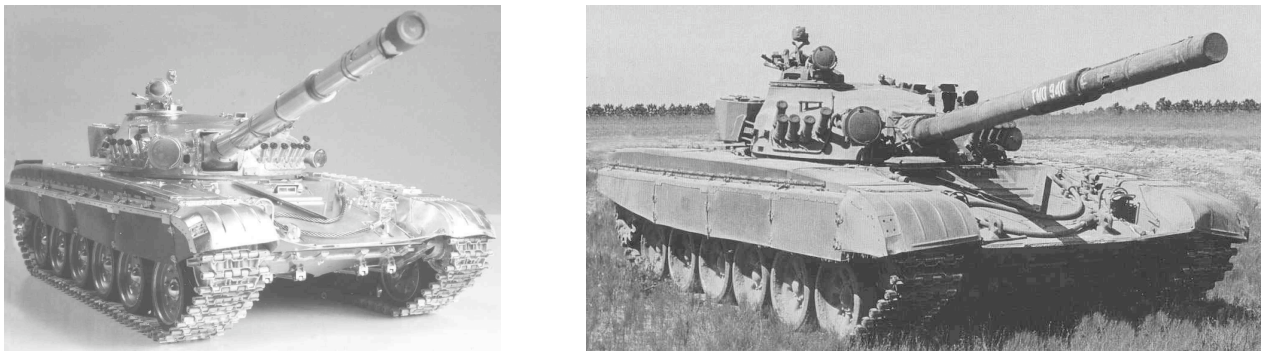

a b

Figure 2. (a) Scale model of the T72 main battle tank (b) the full-scale vehicle on which it was based. Note for example the equivalent deformation on the front fenders.

In addition to the T72 tank models shown in the figures, five additional scale-model main battle tanks were measured. These were the generic version of the Challenger 2, M48, T55, T80, and Leclerc. It has also been useful to compare the measurements taken on the scale-models with those performed at full-scale whenever such data exists. Such a study has been performed at Ka band in Ref [2] and has shown very good agreement. Although there are relatively few full-scale measurements taken at W-band, high quality outdoor turntable data has been taken previously on the T72 by Eglin AFB.[3] This data has been used in this comparison to provide an independent test of the scale-model data. The outdoor turntable data is also listed in Table 2. All data listed in Table 2 are part of the current study, with the exception of the full-scale measurement. The targets were measured under a number of different conditions that include free-space, ground-plane and various turret positions. The simulated ground-plane used in this study modeled arid rough soil.

Target	Replica	Elevation angle	Condition	Turret	Comment	File Number
T72 M1 (#1)	#940	20˚	Free Space	9˚	-5˚ to365˚ azimuth. Taken 9/26/01	1
	#940	20˚	Free Space	9˚	-5˚ to 725˚ azimuth Taken 9/27/01	2
T72 M1(#2)	#940	20˚	Free Space	9˚		3
	#940	20˚	Ground Plane	9˚		4
	#940	20˚	Ground Plane	0˚		5
T72 BK	#747	20˚	Ground Plane	9˚	Reactive Armor	6
T72 Full Scale Measurement	Ref[3]	20˚	Free Space	9˚	High quality full-scale outdoor turntable measurement.	7
Challenger 2	Generic	20˚	Ground Plane	0˚		8
T80	Generic	20˚	Free Space	0˚		9
T55AM2B	Generic	20˚	Ground Plane	0˚		10
M48	Generic	20˚	Ground Plane	0˚		11
Leclerc	Generic	20˚	Ground Plane	0˚		12

Table 2. Data files used in this study. The simulated ground-plane used in this study modeled arid rough soil

3.2. ISAR signature analysis technique.

The data in this study were taken by sweeping the frequency of the system and recording the complex (amplitude and phase) radar return at the sampled frequencies. This was typically done at angular intervals of 0.01˚ or 0.005˚ in order to provide sufficient sampling for the size of the target. The data was then formed into ISAR images by applying a Fast Fourier Transform (FFT) on both the frequency axis and the azimuth axis. The resulting images are suitable for use in a cross correlation algorithm for target identification. Examples of ISAR images for two different MBTs are shown in Figures 4 and 5. These images were formed using the HH polarization and with an FFT over 0.64˚ in azimuth. Each pixel represents the HH intensity, calibrated in dBsm.

The ISAR signature data is analyzed by the standard mathematical 2-D cross correlation described in Ref [4] and implemented in the LabView™ programming language. A detailed description of the technique is presented in Ref [4]. Therefore, only a brief description is given here.

The two ISAR images to be correlated are represented by the functions *f(x,y)* and *w(x,y)*. The sizes of the 2-D arrays are MxN and JxK respectively. The correlation function between the images is,

$$c(s,t) = \sum_x \sum_y f(x,y) w(x - s, y - t) \tag{1}$$

where s=0,1,2,…M-1 and t=0,1,2,…N-1. The sum in Equation(1) is taken over the overlap region between *f(x,y)* and *w(x,y)*. In order to eliminate sensitivity to changes in the amplitudes of *f(x,y)* and *w(x,y)* it is useful to use a normalized version of Equation(1) as is shown in Ref [4]. This yields the correlation coefficient given in Equation(2).

$$\gamma(s,t) = \frac{\sum_x \sum_y \left[f(x,y) - \overline{f}(x,y) \right] \left[w(x - s, y - t) - \overline{w} \right]}{\left\{ \sum_x \sum_y \left[f(x,y) - \overline{f}(x,y) \right]^2 \sum_x \sum_y \left[w(x - s, y - t) - \overline{w} \right]^2 \right\}^{1/2}} \tag{2}$$

where s=0,1,2,…M-1 and t=0,1,2,…N-1, $\overline{w}$ is the average value of pixels in *w(x,y)* (computed only once), and $\overline{f}(x,y)$ is the average value of *f(x,y)* in the current overlap region. It is useful to note that the correlation coefficient function is scaled in the range –1 to 1.

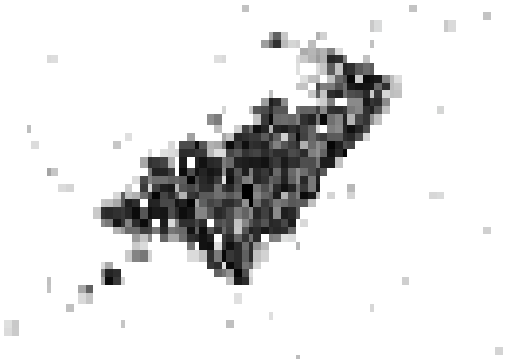

Figure 4. HH ISAR image of T72 Tank at 20˚ elevation and 30˚ azimuth. Image is formed using 0.64˚ integration.

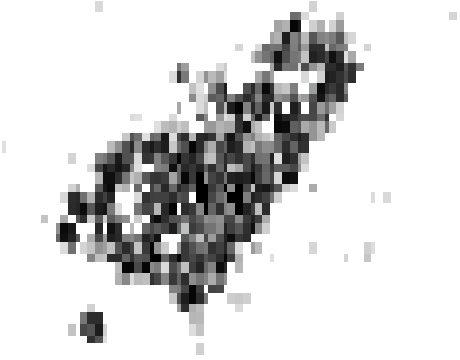

Figure 5. HH ISAR image of T80 Tank at 20˚ elevation and 30˚ azimuth. Image is formed using 0.64˚ integration.

The procedure to test the correlation between two data sets is relatively straightforward. First, the data sets are compared at 0˚, 90˚, 180˚, and 270˚ to register any possible offset in angle between the data sets. While this is seldom necessary for the scale model data, the full-scale outdoor turntable data (Table 2: File 7) did require some correction to ensure the angles were co-aligned. Once angle registration is achieved, ISAR images are formed. A noise threshold is set for the ISAR image. Data points with values below the noise threshold are set to the threshold. The data is represented in units of dBsm. In order to preserve the correct relative weighting of the data points an offset is added to the dBsm values. The offset is equal to the threshold limit described. In this manner, any pixel that falls at or below the threshold will have zero weight. The ISAR images are then correlated using Equation (2). The maximum value of the correlation coefficient is then extracted. This is performed for ISAR images formed at 1˚ increments through the full 360˚ of azimuth rotation. The correlation of one full data set against another therefore produces 360 individual correlation coefficients, one for each ISAR angle. A Probability Density Function (PDF) is then calculated using the 360 correlation amplitudes.

An example of ISAR correlation for the T72 Tank is shown in Figure 6. The data in Figure 6(a), taken in free-space, is used as the template to compare to the data in Figure 6(b), taken on the ground plane. Figure 6(c) shows the best match region of Figure 6(b). Figure 6(d) shows the remainder after the best match region of Figure 6(c) is removed from the original test image Figure 6(b). The maximum correlation amplitude for the comparison of these images was 0.87. Throughout the discussion of the results the correlation amplitudes will be expressed in percentage of the maximum possible amplitude, a value of 1 for a perfect match. For example, the correlation amplitude of 0.87 will then be referred to as 87%. Figure 7 shows the results of data Files (1) and (4) from Table 2 correlated through the full 360˚ azimuth angle. These data sets were taken with the T72 in free space and on the ground plane, respectively. Figure 7(a) shows the maximum correlation probability. Figure 7(b) shows a typical PDF that is generated from the data in Figure 7(a), which shows an 87% correlation amplitude.

(a) Template Image (b) Test Image (c) Best Match Region (d) Remainder

Figure 6. T72 HH ISAR correlation at 20˚ depression and 30˚ azimuth. Image is formed using 0.64˚ FFT.

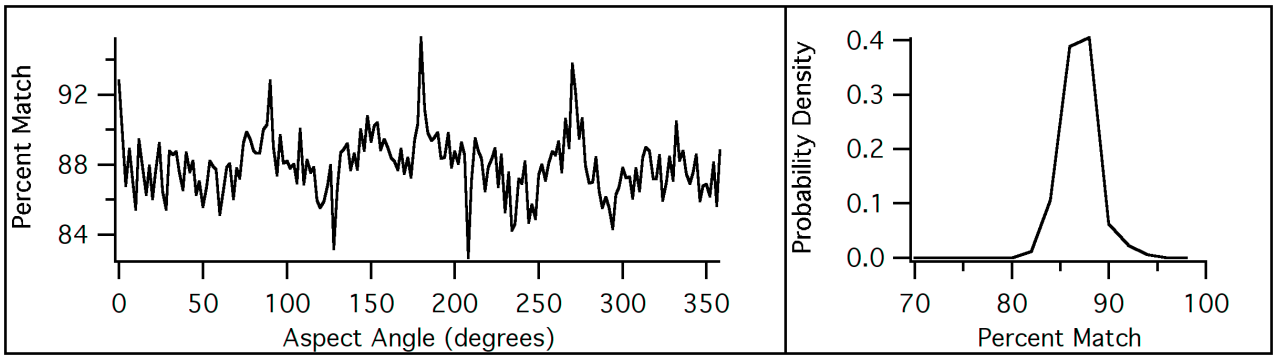

a b

Figure 7. Typical Correlation plots. (a)Correlation percentages for the 360˚ of data using images spaced every degree. (b)PDF of the data in (a). Data from Files #1 and #4 were correlated in HH polarization.

3.3. Correlation results.

The results for the cross correlation of the data sets in Table 2 using the HH polarization state are shown in the figures below. Figure 8 shows the PDF results of the T72 data correlated with several other T72 data sets. The ISAR images were generated using a 0.64˚ FFT in azimuth and a –30dBsm noise threshold. The legend in the figure is labeled with the file numbers from Table 2 in parentheses and a description of the data file. It is useful to note in this figure that data set (2) which contained two full spins of the target shows the largest correlation when the first 360˚ are compared to the second 360˚. The second highest correlation is observed when file (1), containing T72 free-space data, is compared with file (4), which contains the data taken on a ground plane. A comparison of the target with the turret pointing forward at 0˚ vs. the turret rotated to 9˚ has the next highest value. The comparison of the T72 tanks with and without reactive armor shows the smallest correlation. This is perhaps not surprising since the reactive armor changes the scattering on the tank significantly. It is also interesting that changing the turret by 9˚ has only a modest effect on the correlation amplitude. This may be an indication that for this tank, the majaroity of the scattering occurs from features on the body of the tank rather than from the turret.

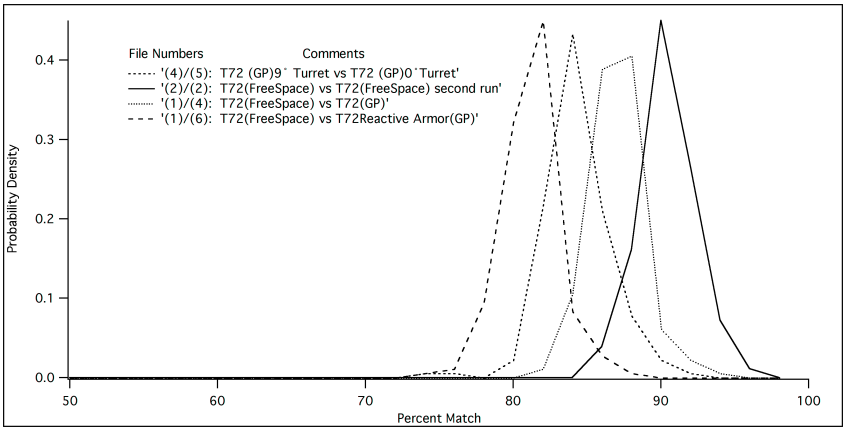

Figure 8. PDF results for the correlation of several T72 data sets.

Additional results for the correlation of the data sets listed in Table 2 are shown in Figures 9, 10 and 11. The figures show PDFs for the correlation of T72 data sets in free-space compared with other T72 data and with data taken on other MBTs. The results are separated into two classes for easier display. In the upper part of each figure the correlation results are shown for the T72 compared to other T72 data sets. The lower part of each figure shows the correlation results against the other MBTs. While the same data set combinations are used in Figures 9-11, the data was correlated using different ISAR images. This was done in order to determine the effect this would have on the template

and test images. The results in Figure 9 were analyzed using a 0.64˚ FFT to form the ISAR image for both the test and template image. The results in Figure 10 were obtained in a similar manner but a 5.12˚ FFT was used for the formation of ISAR images. The data for Figure 11 were analyzed by a combination technique where a 0.64˚ FFT was used for the test image and a 5.12˚ FFT was used for the template image. The cross-range pixels in the template image were then incoherently summed in groups of 8 in order to form a template with the same cross-range resolution as the test file but with information distributed over 5.12˚.

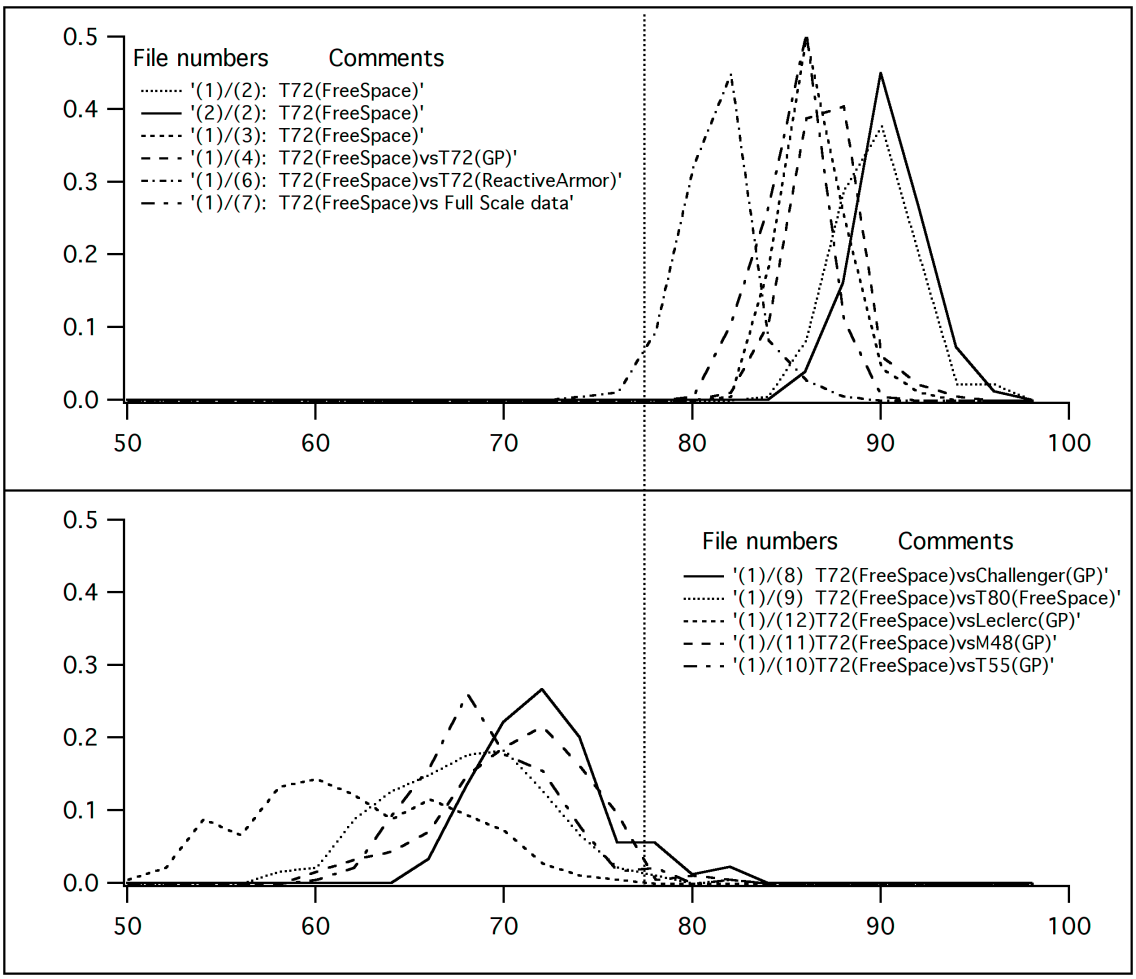

Figure 9. HH PDF results for comparison of ISAR data from Table 2 using 0.64˚ FFT image formation.

A comparison of the upper and lower graphs in Figure 9 shows a general trend that separates the results for similar MBTs from those of different MBTs. The upper curves of Figure 9 show the PDFs of the T72 were well correlated with other T72 data sets. It is useful to note that the PDFs showing the highest correlation are combinations of Files 1 and 2 that were taken to provide a baseline result for data sets with the smallest possible differences. The data in File 1 was collected through 370˚ of azimuth. The target was removed and then remounted on the pylon before the system was re-calibrated. In File 2 data was collected for a full 730˚ of azimuth (-5˚ to 725˚). The data from the first 360˚ was compared to that of the second 360˚ of azimuth. As expected, these files show the highest correlation and their PDFs lay nearly on top of each other. Correlation between Files (1) and (3) and Files (1) and (4) show the next highest results. These are correlations between different models of the same T72. These figures show only a small decrease in the median PDF demonstrating the high reproducibility of the models. It is also very interesting to note that a correlation of File (1) with File (7) (which contains data on the full-scale vehicle using an outdoor range) gives a result that is virtually the same as the PDF of Files (1) and (3). This demonstrates the high fidelity of the scale models, the robustness

of the algorithm, and the ability to correlate results from entirely different radar systems. Finally, the correlation of the T72BK, which has reactive armor and the T72M1, without reactive armor shows the largest drop in median PDF. This is to be expected, since the reactive armor does significantly change the scattering. But the change is small enough for the target to remain identifiable as a T72.

The results for the correlation of the T72 data sets with those of different MBTs is shown in the lower graph of Figure 9. The data show a general trend of lower correlation values when different MBTs are compared, and the PDF distribution becomes irregular with a smaller maximum value. In previous studies at Ka-band[2] the T80 data set was seen to correlate almost as well with the T72M1 as the T72BK data set with reactive armor. This is not the case at here, where the graph shows the T80 PDF well separated from that of the T72 with reactive armor. It is interesting to note that the MBT displaying the highest correlation when compared to the T72 was the Challenger 2. This is somewhat surprising since the Challenger 2 is physically larger than the T72, but since the Challenger 2 displays a significant amount of complex scattering, there would be a greater chance for coincidental spatial correlation under these conditions.

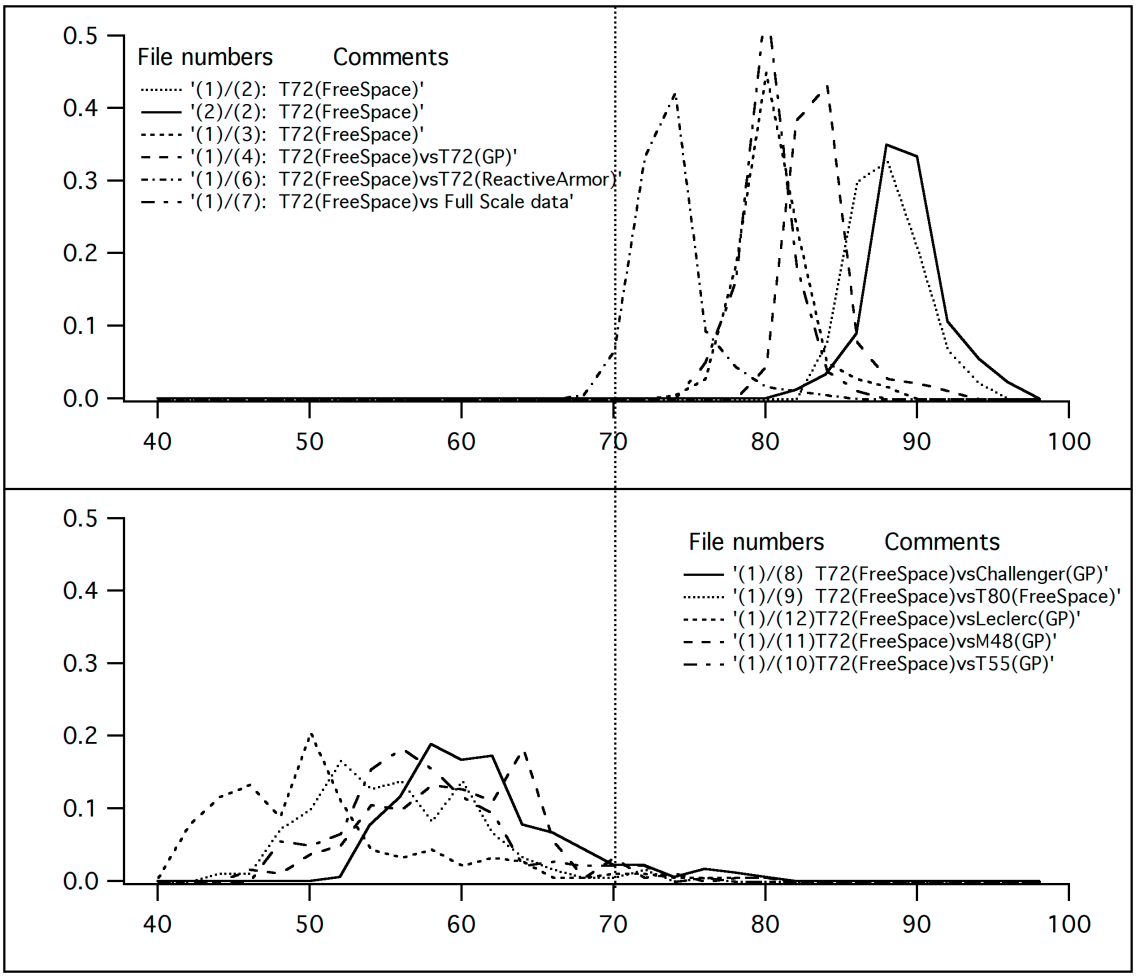

Figure 10. HH PDF results for comparison of ISAR data from Table 2 using 5.12˚ FFT image formation.

Figures 10 and 11 show similar plots for comparison of the same data sets used in Figure 9. The correlation was carried out using different ISAR image formation for the template and test images. The effect of using a 5.12˚ FFT to form the ISAR images is seen in Figure 10, which shows that the wider ISAR image formation helps to separate the data sets further. The most significant effect is seen in the upper graph of Figure 10 where the higher cross-range

resolution allows the correlation to better distinguish between the different T72 data sets. The correlations for different MBTs in the lower graph also tends to show better separation.

The PDFs displayed in Figure 11 show the results of a correlation of images formed using a 5.12˚ FFT for the template image and a 0.64˚ FFT for the test image. This was done to observe the effect on the correlation when templates containing information across a large angular extent are compared to test images formed over smaller angular integrations. Since ISAR images at W-band are typically formed using an FFT over only 0.5˚ in azimuth, a large number of ISAR images might be required in order to provide complete data coverage when forming a comprehensive ATR template library. It is thought that this simple technique might be useful in creating a template image with the correct resolution and containing the information from a very large angular extent. This would not only reduce the number of template images required to provide complete coverage but would make the comparison less sensitive to small azimuth misalignments of the data sets. Figure 11 shows that, although the T72 data sets are still separable from those of the different MBTs, there is less separation. It is interesting to note that the various T72 data sets in the upper graph of Figure 11 have now become virtually indistinguishable and the PDF of the Challenger 2 is now overlapping with the PDF for the T72 with reactive armor. However, this comparison does show that this template image does produce enough separation to distinguish the T72 from other MBTs, but at the cost of loosing some ability to distinguish different types of T72s.

Figure 11. HH PDF results for comparison of ISAR data from Table 2 using 0.64˚ FFT image formation for the test image and a 5.12˚ FFT for the template image.

4. Summary

The cross-correlation of scale-model signatures between seven MBTs has been explored through the use of 20-degree elevation ISAR imagery. Target seperability is seen between the data taken on the scale-model T72 MBT and the data sets taken on the scale-model Challenger 2, T55, T80, M48 and Leclerc MBTs. The scale model T72 ISAR data has also been compared to full-scale measurements and have demonstrated good correlation results. Several different template images have been used in the HH polarization. Work is currently being done on templates using circular polarization. Data sets at very high elevation angles are also being studied for targets both in free-space and on simulated ground terrain.

REFERENCES

1. T. M. Goyette, J. C. Dickinson, J. Waldman, W. E. Nixon, and S. Carter, "Fully polarimetric W-band ISAR imagery of scale-model tactical targets using a 1.56-THz compact range", *Proceedings of SPIE, Algorithms for Synthetic Aperture Radar Imagery VIII*, Vol. **4382**, p229-240, 2001.
2. R. H. Giles, W. T. Kersey, M. S. McFarlin, R. Finley, H. J. Neilson, and W. E. Nixon, "A Study of Target Variability and Exact Signature Reproduction Requirements for Ka-Band Radar Data", *Proceedings of SPIE, Signal Processing, Sensor Fusion and target Recognition X*, Vol **4380**, p117-126, 2001.
3. Private Communication to the authors.
4. R. C. Gonzalez and R. E. Woods, *Digital Image Processing*, p583-584, Addison-Wesley Publishing, Reading Massachusetts, 1992.